Comparison of a quantum error-correction threshold for exact and approximate errors

Mauricio Gutiérrez and Kenneth R. Brown*

Schools of Chemistry and Biochemistry; Computational Science and Engineering; and Physics, Georgia Institute of Technology, Atlanta, Georgia 30332-0400, USA

(Received 4 January 2015; published 27 February 2015)

Classical simulations of noisy stabilizer circuits are often used to estimate the threshold of a quantum error-correcting code. Physical noise sources are efficiently approximated by random insertions of Pauli operators. For a single qubit, more accurate approximations that still allow for efficient simulation can be obtained by including Clifford operators and Pauli operators conditional on measurement. We examine the feasibility of employing these expanded error approximations to obtain better threshold estimates. We calculate the level-1 pseudothreshold for the Steane [[7,1,3]] code for amplitude damping and dephasing along a non-Clifford axis. The expanded channels estimate the actual channel action more accurately than the Pauli channels before error correction. However, after error correction, the Pauli twirling approximation yields very accurate estimates of the performance of quantum error-correcting protocols in the presence of the actual noise channel.

DOI: 10.1103/PhysRevA.91.022335 PACS number(s): 03.67.Pp, 03.65.Yz

I. INTRODUCTION

The threshold theorem of quantum error correction promises the accurate implementation of arbitrary size quantum algorithms if the underlying physical errors are below certain values. The error thresholds depend strongly on the specific quantum error correcting code, how errors are detected and fixed [1–3], and what errors are assumed [4–7]. Most codes have been designed to fix random Pauli errors and error correction procedures can be simulated efficiently using the stabilizer formalism [8,9]. A broader class of errors including Clifford operations [10] and Pauli measurements [11] can also be included in this formalism. For a single qubit, this extended error set has been shown to yield improved approximations of realistic error models including amplitude damping [11].

Here we examine whether these improved approximations also lead to more accurate threshold estimates. Specifically, we calculate the level-one pseudothreshold for the Steane [[7,1,3]] code [12] for two nonstabilizer errors, amplitude damping and a depolarization channel along a magic-state axis, and compare the exact solution to approximations based on Pauli errors or Clifford and Pauli measurement errors. The Steane code has been well studied theoretically [13–19] and a logically encoded state has been recently demonstrated experimentally [20]. The code is small enough to allow for exact simulation similar to recent work on distance-3 surface codes, which compared a realistic error model corresponding to T_1 (amplitude damping) and T_2 (dephasing) processes and an approximate Pauli error model based on twirling [6].

In addition to the pseudothreshold, we are interested in two other qualities of the approximation, the accuracy and the honesty. The accuracy is a measure of how close is the state generated by the approximate evolution to the state generated by the exact evolution. We describe an approximation as honest if the final state after the approximate evolution is further from the initial state than the final state after the exact evolution. In other words, an approximation is honest if it upper-bounds the error of the exact evolution. As pointed out by Puzzuoli *et al.* the composition of honest approximations is not necessarily honest [21]. This implies that an approximation that is honest at the one-qubit physical level might lead to a dishonest representation of the overall error produced on the system. As our goal is to employ our approximate channels to infer the performance of error-correcting strategies under realistic nonstabilizer noise, we need to be sure that they compose in an honest fashion. We provide numerical evidence that, in the context of an error-correcting circuit, an honest approximation at the physical level remains honest at the logical level. Furthermore, we show that, for the error models studied, physically dishonest approximations based on the Pauli channel might lead to approximations at the logical level that are both approximately honest and very accurate, in agreement with similar results obtained by Geller and Zhou [22]. This suggests that it might not be necessary for the approximations to be honest at the physical level.

The paper is organized as follows. In Sec. II, we describe the realistic error channels and our method to approximate them [11]. In Sec. III, we review the important concepts of honesty and accuracy of an approximate channel. In Sec. IV we explain our procedure for calculating the pseudothresold. In Sec. V, we present our results before concluding in Sec. VI.

II. ERROR CHANNELS

We review all the error channels introduced in Ref. [11]. We start with the stabilizer expansions to the Pauli channel (PC) that are used as models to approximate realistic nonstabilizer error channels. Next, we discuss two important error channels that lie outside the stabilizer formalism. Finally, we review two different constraints under which the approximations are performed. All the error channels introduced in this section will be expressed in the operator-sum representation.

Throughout the paper we use X, Y, and Z to represent the Pauli matrices with associated eigenvectors $\{|+\rangle,|-\rangle\}$, $\{|+i\rangle,|-i\rangle\}$, and $\{|0\rangle,|1\rangle\}$, respectively.

*ken.brown@chemistry.gatech.edu

 ©2015 American Physical Society

A. Efficiently simulatable processes

One of the main ideas introduced in [11] was that the PC can be greatly expanded without becoming nonstabilizer. We do this by adding Kraus operators that correspond to either Clifford operations or Pauli measurements followed by conditional Pauli operations. For the one-qubit case, the Clifford channel (CC), which corresponds to the first expansion, is composed of the 24 operators that maintain the symmetry of the chiral Clifford octahedron [23]. Another expansion to the PC can be obtained by introducing pairs of operators that effectively produce a measurement in a Pauli basis followed by a conditional Pauli operation, such that all states are mapped to the same state. We refer to these pairs of operators as measurement-induced translations. For each Pauli state, $|\lambda\rangle$, these operations can be represented by the following pairs:

$$\{E_{\lambda 0} = |\lambda\rangle\langle\lambda|, E_{\lambda 1} = |\lambda\rangle\langle\lambda^{\perp}|\}. \tag{1}$$

The addition of these measurement-induced translations to the PC gives rise to the Pauli + measurements channel (PMC), while their addition to the CC produces the Clifford + measurements channel (CMC).

B. Nonstabilizer error channels

As in [11], we use the efficiently simulatable channels to approximate realistic nonstabilizer channels. In particular, we focus on the amplitude damping channel (ADC) and the polarization along an axis in the x-y plane of the Bloch sphere (Pol$_\phi$C), shown on Eqs. (2) and (3), respectively:

$$\mathrm{ADC} = \begin{cases} E_{A0} = |0\rangle\langle 0| + \sqrt{1-\gamma}\,|1\rangle\langle 1| \\ E_{A1} = \sqrt{\gamma}\,|0\rangle\langle 1|, \end{cases} \tag{2}$$

$$\mathrm{Pol}_\phi\mathrm{C} = \begin{cases} E_{xy0} = \sqrt{1-p_\phi}\,I \\ E_{xy1} = \sqrt{p_\phi}\,[\cos(\phi)\,X + \sin(\phi)\,Y]. \end{cases} \tag{3}$$

C. Constraints

The free parameters in the PC and its expansions correspond to the probabilities associated with the Kraus operators. Previously, we have obtained stabilizer approximations to the realistic nonstabilizer channels by minimizing the Hilbert-Schmidt distance [24,25] over the parameter space of the models. As we do not want to underestimate the deleterious effect of the target channel on quantum information (i.e., we want our approximation to be honest [10]), we perform the minimizations such that the approximate channels constitute an upper bound on the error induced on the system. Mathematically, this condition can be enforced in a variety of ways by employing different fidelity or distance measures. From the constraints that we have studied, the most lenient corresponds to the average fidelity constraint, in which we enforce the following condition:

$$F_{\mathrm{av}}(I,\mathrm{target}) \geq F_{\mathrm{av}}(I,\mathrm{model}). \tag{4}$$

The average fidelity between a unitary transformation V and a quantum channel K is given by:

$$F_{\mathrm{av}}(V,K) = \frac{1}{N^2}\sum_i |\mathrm{Tr}(V^\dagger K_i)|^2, \tag{5}$$

where N is the dimension of the Hilbert space and $\{K_i\}$ are the Kraus operators of the error channel K. On all the approximations that we have performed, the average fidelity constraint has always given the same results as if no constraint had been applied.

On the other hand, the most stringent constraint corresponds to the worst trace distance, which enforces that the trace distance between an initial pure state and the final state generated from the model approximations cannot be smaller than the trace distance between the initial state and the target transformation:

$$D^{\mathrm{Tr}}(\rho,\mathrm{target}(\rho)) \leqslant D^{\mathrm{Tr}}(\rho,\mathrm{model}(\rho)), \tag{6}$$

where the trace distance is calculated using the following expression:

$$D^{\mathrm{Tr}}(\rho,\sigma) = \tfrac{1}{2}\mathrm{Tr}|\rho-\sigma|. \tag{7}$$

This worst trace distance constraint results in approximate channels that are honest, in the sense that the deleterious effect of the target error channel on any pure quantum state will never be underestimated, as pointed out by Magesan *et al.* [10] and Puzzuoli *et al.* [21]. We could think of an even tighter constraint in which we enforce this condition on every initial state, pure or mixed. However, if the target and the model transformations have different fixed points, this condition is impossible to satisfy. We compare results for both constraints and label them "A" (average fidelity constraint) and "W" (worst trace distance constraint).

III. HONESTY AND ACCURACY AT THE PHYSICAL AND LOGICAL LEVELS

For each approximate channel, we study two properties: honesty and accuracy. An approximate channel is honest if it does not underestimate the detrimental effect of the target error channel. The accuracy of an approximate channel refers to how closely it can mimic the effect of the target channel on an initial state. More explicitly, if a target error channel E maps a pure state ρ to $E(\rho)$ and an approximate channel A maps the same state to $A(\rho)$, then A is honest if

$$D^{\mathrm{Tr}}(\rho,E(\rho)) \leqslant D^{\mathrm{Tr}}(\rho,A(\rho)) \tag{8}$$

for every pure state in the initial physical or logical space. The accuracy is measured by the average trace distance between the resulting states:

$$\langle D^{\mathrm{Tr}}(E(\rho),A(\rho))\rangle. \tag{9}$$

Notice that for both properties, our measure of choice is the trace distance. A good approximate channel will be honest (or as least dishonest as possible) and as accurate as possible, not only at the physical level, but also at the logical levels. We distinguish four different scenarios to compare honesty and accuracy: (i) the physical (one-qubit) level, (ii) the uncorrected logical level, (iii) the logical level with perfect EC, and (iv) the logical level with faulty EC, as depicted in Fig. 1.

For each target non-Clifford error channel, we study two kinds of approximations: (i) the Pauli channels (PC), which employ only one-qubit Pauli operators, and (ii) the expanded channels or Clifford + measurements channels (CMC), which include all the one-qubit Clifford operators

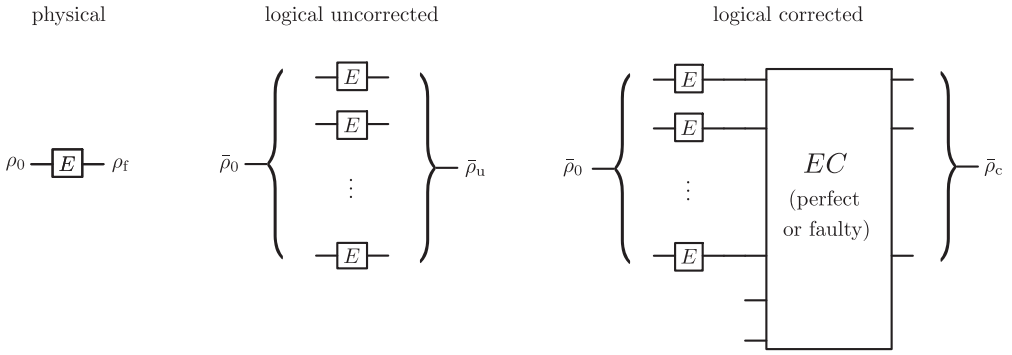

FIG. 1. We study the honesty and accuracy of the approximate channels at the physical level and at the logical level before and after error correction. The logical initial state is encoded without errors and then errors are applied. The preparation of the ancillary cat state in the faulty EC is error-free as well, as shown in Fig. 2.

and the measurement-induced translations [11]. In turn, each kind of approximation is performed with the average fidelity constraint (A) and the worst trace distance constraint (W), resulting in four approximate channels. Notice that the unconstrained PC is equivalent to the Pauli twirled approximation [10,21,22], the channel obtained by removing the off-diagonal elements from the target channel's process matrix in the Pauli basis [26]. We also analyze the completely isotropic Pauli channel or depolarizing channel (DC), the most common error model used when calculating thresholds. In this paper we are comparing single-qubit error channels and we only use the single-qubit depolarizing channel. This channel is a version of the PCa where the coefficients corresponding to each Pauli matrix are forced to have the same value. This error model serves as a reference. The approximations are summarized in Table I.

IV. CALCULATION OF THE PSEUDOTHRESHOLD

Our objective with respect to the pseudothreshold is twofold. On the one hand, we want to study how sensitive a QECC's threshold is to the noise model. On the other hand, we want to determine if the thresholds obtained with our expanded error models approximate the realistic threshold more accurately than the PC.

A. Procedure to compute the level-one pseudothreshold

Because our target error models are nonstabilizer, we perform exact (full density matrix) simulations of quantum error correction (QEC) circuits up to the first level of encoding. We calculate a particular QEC code's level-one pseudothreshold under a given error channel in the following way:

(i) Run the physical circuit:
  (a) Choose an initial 1-qubit pure state, $|\psi\rangle$.
  (b) Apply the selected error channel.
  (c) Compute the fidelity between the initial and final states.

(ii) Run the logical circuit:
  (a) Encode the initial state using the selected QECC.
  (b) Apply the error channel to each physical qubit.
  (c) Perform EC.
  (d) Compute the fidelity between the initial and final logical states.

We are interested in how much the final state is affected by errors which are uncorrectable by the selected QECC. Therefore, for the case with faulty corrections, we perform one round of perfect EC before computing the fidelity. This has the effect of eliminating correctable errors, which happened during or after the faulty EC. The process of performing a round of perfect EC and then computing the fidelity can also be viewed as computing an error-corrected fidelity:

$$F_{\mathrm{EC}}(|\psi_L\rangle,\rho_L) = \sqrt{\sum_i \langle\psi_L|E_i^\dagger P_i^\dagger \rho_L P_i E_i|\psi_L\rangle}, \qquad (10)$$

where $|\psi_L\rangle$ is the initial logical state and ρ_L is the final logical state, which, in general, will not be pure. The set $\{E_i\}$ consists of all error operators which the QECC is designed to correct, while $\{P_i\}$ is the set of projectors to the subspaces associated with each error. For the Steane [[7,1,3]] code, the set $\{E_i\}$ is formed by the 64 Pauli operators formed by all possible combinations of X and Z errors acting independently on at most one qubit and includes the identity operator for the case of no errors.

(iii) Repeat steps (i) and (ii) for various noise strengths to obtain fidelities for the physical and logical circuits. The threshold is given by the first intersection between the two curves.

(iv) Repeat this procedure for several initial states to obtain an average threshold. For the perfectly corrected case, we select 80 initial points uniformly distributed on the Bloch sphere. For the faultily corrected case, we select 20.

Notice that our logical unit consists of a logical identity gate, which is always faulty, and an EC step, which may or

TABLE I. Summary of the various target and approximate channels.

Channel	Complete name	Honesty constrained
ADC	amplitude damping	–
$\mathrm{Pol}_\phi\mathrm{C}$	polarization along non-Clifford axis	–
PCa	Pauli	no
PCw	Pauli	yes
CMCa	Clifford + measurements	no
CMCw	Clifford + measurements	yes
DC	Depolarizing channel	no

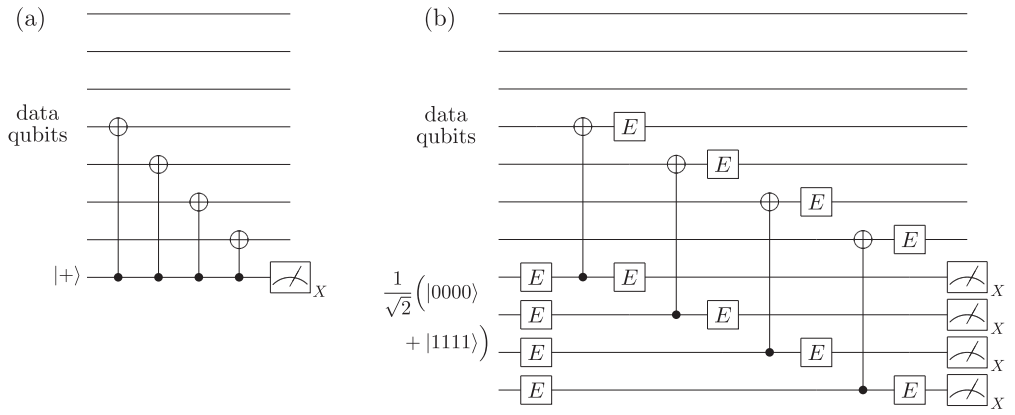

FIG. 2. Circuits representing the measurement of the operator $IIIXXXX$ in (a) an error-free regime and (b) a faulty regime. In the former case, we only need to employ 1 ancillary qubit. Notice that the ancillary qubit starts in the $|+\rangle$ state and the measurement is performed in the X basis. In the faulty EC regime, in order to make the procedure fault tolerant, we employ four ancillary qubits initialized in a cat state [29]. We then measure each ancillary qubit in the X basis and compute their parity to extract the outcome.

may not be faulty. This logical unit is often referred to as a simple rectangle, in contrast to an extended rectangle, where the logical gate is inserted between two EC steps [27,28]. The qualitative trends of the resulting pseudothresholds should remain unchanged between a simple and an extended rectangle.

B. Methods of error correction

The EC step is performed by measuring the stabilizer generators and later correcting any detected errors. We distinguish between the error-free EC, which results in a code-capacity pseudothreshold, and the faulty EC, which results in the more realistic circuit-based pseudothreshold. The faulty EC is built by inserting an error channel after each gate in the original circuit. As the Steane code will be the focus of our analysis, consider, for example, the measurement of the stabilizer $IIIXXXX$, as depicted in Fig. 2. The error-free EC step would consist of circuits analogous to Fig. 2(a) for each stabilizer generator. On the other hand, in the faulty EC regime, each stabilizer generator would be measured as shown in Fig. 2(b). Each stabilizer measurement is then repeated and the syndrome is compared to the one in the previous round. If there is a disagreement between these two, a third round of stabilizer measurements is performed and its syndrome is selected as the definitive one.

V. RESULTS

A. Honesty and accuracy of the approximations

By construction, the W approximations are honest at the physical (one-qubit) level, provided that the initial state is pure. In our previous work we also determined that, when approximating a general non-Clifford channel at the physical level, the expanded channels are more accurate than the Pauli channels. Before computing the level-one pseudothresholds for different approximations, we first examine if the honesty of the W approximations and the greater accuracy of the expanded channels were maintained at the logical level.

1. Amplitude damping channel (ADC)

For the physical, logical uncorrected, and logical with perfect EC levels, we have selected 80 initial states uniformly distributed over the Bloch sphere surface. For the logical faultily corrected level, we have selected 20 points, because the simulations involve three extra qubits and consequently take an exponentially longer time. We have computed the trace distance between each initial state and the resulting final state after the ADC and its approximations. The average distances are shown in the first row of Fig. 3 as a function of the damping strength, γ. Likewise, we have computed the trace distance between each final state after the ADC and each final state after every approximate channel. The average distances are presented in the second row of Fig. 3. The behavior in the limit of small damping strength ($\gamma \to 0$) is summarized in Tables II and III. In this limit, it is useful to Taylor-expand the distances in terms of the noise strength and compare the coefficients of the leading-order terms. Expectedly, for the corrected logical cases the linear term is suppressed and the leading order is quadratic. For the physical and uncorrected logical cases, the leading order is linear. At the logical level with faulty EC, simulations were only carried out at low damping strengths ($\gamma \in [10^{-5}, 10^{-3}]$), which is the pertinent region for the pseudothreshold computation.

Notice that at the physical level in the first row of Fig. 3, the W approximations result in curves that are above the target ADC by construction, while the a approximations produce curves below it. This behavior is also present in the small noise strength limit, as can be seen by the magnitudes of the linear coefficients (Table II): PCa $<$ CMCa $<$ ADC $<$ CMCw $<$ PCw. Likewise, the accuracies of the CMC approximations are much better than that of the PC approximations (Table III). In the $\gamma \to 0$ limit, the CMC approximations are $\approx$3 times more accurate.

At the three logical levels, the W approximations are honest for every damping strength. This is true not just on average, but for every initial state considered. This is an important result, as it means that we can safely use the W approximations as a substitute of the ADC when determining codes' thresholds or other error-correcting properties. Remarkably, the dishonesty

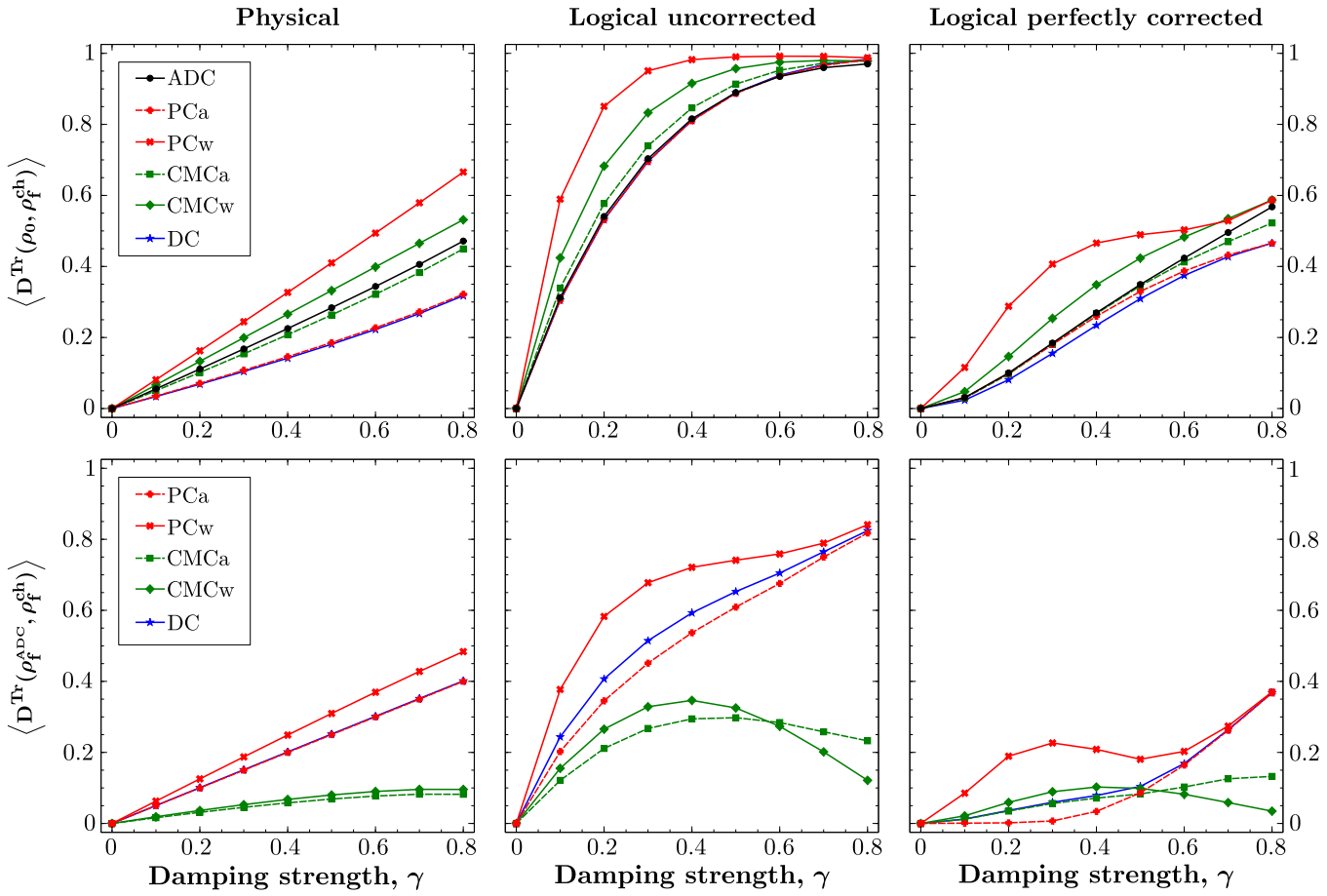

FIG. 3. (Color online) Distances used to assess the honesty (top row) and accuracy (bottom row) of the approximate channels to the ADC at various levels.

TABLE II. Honesty of the approximate channels to the ADC in the limit of small damping strength. Standard deviations below 10^{-9} are not reported.

Channel	Physical D^{Tr}/γ	Logical uncorrected D^{Tr}/γ	Logical perfectly corrected D^{Tr}/γ^2	Logical faultily corrected $D^{\mathrm{Tr}}/(10^2\gamma^2)$
ADC	0.55(27)	3.62	3.76(96)	8.0(1.8)
PCa	0.347(79)	3.50	3.76(96)	7.8(1.8)
PCw	0.81(12)	8.35	18.5(3.5)	37.7(8.0)
CMCa	0.50(18)	4.00	3.48(45)	6.3(1.2)
CMCw	0.66(24)	5.33	6.19(80)	11.3(2.2)
DC	0.333	3.50	2.75(36)	4.95(96)

TABLE III. Accuracy of the approximate channels to the ADC in the limit of small damping strength. Standard deviations below 10^{-9} are not reported.

Channel	Physical D^{Tr}/γ	Logical uncorrected D^{Tr}/γ	Logical perfectly corrected D^{Tr}/γ^2	Logical faultily corrected $D^{\mathrm{Tr}}/(10^2\gamma^2)$
PCa	0.500	2.41	$7(12) \times 10^{-6}$	0.123(28)
PCw	0.63(26)	4.94	14.8(2.6)	29.8(6.2)
CMCa	0.166(60)	1.35	1.61(44)	2.15(74)
CMCw	0.194(60)	1.75	3.05(94)	3.7(1.1)
DC	0.505(97)	2.92	1.68(69)	3.2(1.2)

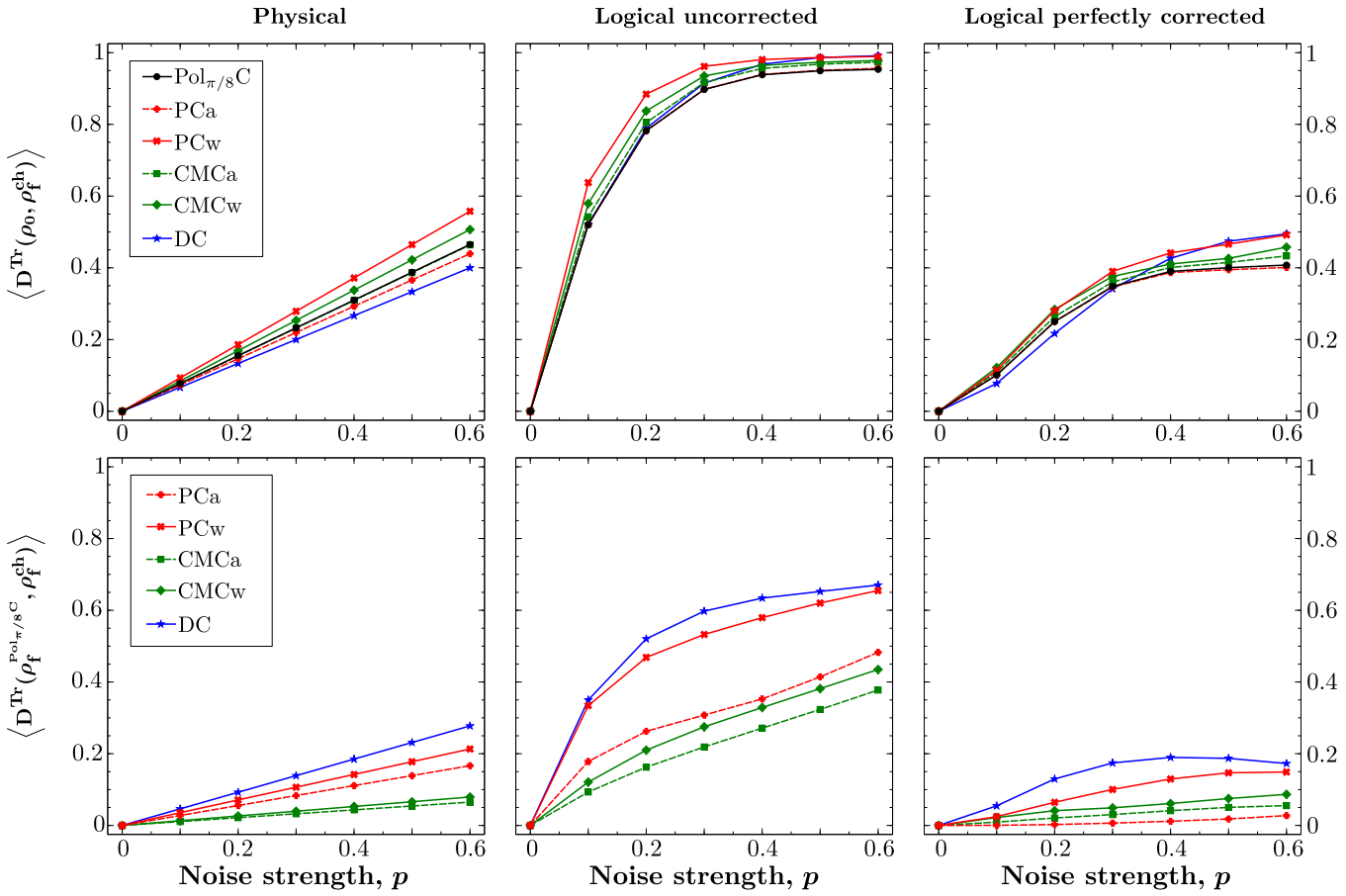

FIG. 4. (Color online) Distances used to assess the honesty (top row) and accuracy (bottom row) of the approximate channels to the $\mathrm{Pol}_{\pi/8}\mathrm{C}$ at various levels.

of the PCa is greatly reduced from the physical to the logical levels in the limit of small γ. Its error is below the honesty cutoff by 36% at the physical level but by less than 2% for both corrected logical levels and well within the deviation in the distance. In contrast, the dishonesty of the CMCa is not improved at the logical levels and is below the honesty cutoff by 8–20% for all cases.

The variation of the accuracy from level to level shows an interesting behavior. For both levels where the effect of the errors is linear (physical and uncorrected logical), in general the CMC channels and the a approximations are more accurate than the PC channels and the W approximations, respectively. This is seen by the magnitudes of the linear coefficients (Table III): CMCa < CMCw < PCa < PCw. At the logical level with perfect EC, this intuitively expected behavior is seen only for high damping strengths ($\gamma > 0.5$) (see Fig. 3). Surprisingly, for lower damping strengths, the most accurate approximation is given by the unconstrained PC, as can be observed by the suppression of the second order terms in the accuracy (Table III). This behavior is particularly pronounced at the logical level with perfect EC, where the second-order terms for the PCa and ADC are practically indistinguishable.

TABLE IV. Honesty of the approximate channels to the $\mathrm{Pol}_{\pi/8}\mathrm{C}$ in the limit of small noise strength. Standard deviations below 10^{-9} are not reported.

Channel	Physical D^{Tr}/p	Logical uncorrected D^{Tr}/p	Logical perfectly corrected D^{Tr}/p^2	Logical faultily corrected $D^{\mathrm{Tr}}/(10^3 p^2)$
$\mathrm{Pol}_{\pi/8}\mathrm{C}$	0.78(24)	7.00	16.2(4.7)	2.22(72)
PCa	0.73(20)	7.00	16.2(4.7)	2.22(72)
PCw	0.93(18)	9.47	18.5(4.9)	2.71(77)
CMCa	0.77(22)	7.41	17.8(5.1)	2.67(83)
CMCw	0.84(23)	8.17	20.8(5.9)	3.12(96)
DC	0.667	7.00	11.0(1.4)	1.82(35)

TABLE V. Accuracy of the approximate channels to the $\mathrm{Pol}_{\pi/8}\mathrm{C}$ in the limit of small noise strength. Standard deviations below 10^{-9} are not reported.

Channel	Physical D^{Tr}/p	Logical uncorrected D^{Tr}/p	Logical perfectly corrected D^{Tr}/p^2	Logical faultily corrected $D^{\mathrm{Tr}}/(10^2 p^2)$
PCa	0.278(82)	2.47	$6.1(7.7) \times 10^{-6}$	$5.8(1.6) \times 10^{-5}$
PCw	0.36(21)	4.95	3.8(1.1)	6.2(1.6)
CMCa	0.108(25)	1.09	1.76(41)	4.7(1.0)
CMCw	0.132(43)	1.37	4.6(1.1)	9.2(2.4)
DC	0.46(11)	4.67	9.2(1.3)	9.7(1.5)

2. *Polarization along a non-Clifford axis channel* ($\mathrm{Pol}_\phi\mathrm{C}$)

We perform an analogous analysis for our second target error channel: the polarization along a non-Clifford axis on the X-Y plane of the Bloch sphere. We select the axis forming an angle $\phi = \pi/8$ with respect to the X axis, as this is the angle for which the expanded error models perform the worst [11]. Once again, we have selected 20 initial states for the faultily corrected level and 80 points for all other levels. We have computed the trace distance between each one of them and the resulting final state after the $\mathrm{Pol}_{\pi/8}\mathrm{C}$ and its approximations. The average distances are shown in the first row of Fig. 4 as a function of the noise strength, p. Likewise, we have computed the trace distance between each final state after the $\mathrm{Pol}_{\pi/8}\mathrm{C}$ and each final state after every approximate channel. The average distances are presented in the second row of Fig. 4. The behavior in the limit of small noise strength ($p \to 0$) is summarized in Tables IV and V. As for the ADC, at the physical and uncorrected logical levels, the leading order is linear. At the corrected logical levels, the leading order is quadratic.

As observed on the ADC, the W approximations are honest at every level and for every noise strength. This holds in the average case and also for each initial state considered. Interestingly, the CMCa becomes honest on average and the PCa average distances are indistinguishable from honest.

Notice that, just like for the ADC, at the physical and uncorrected logical levels, the CMC channels and the A approximations are more accurate than their counterparts PC and W, respectively. This can be seen by the magnitudes of the linear coefficients (Table V): CMCa < CMCw < PCa < PCw. At the physical level, and in the $p \to 0$ limit, the CMC approximations are $\approx$3 times more accurate than the PC approximations. At the corrected logical levels, the most accurate approximation is once again given by the PCa. Surprisingly, this behavior holds even up to high noise strengths ($p = 0.6$). In the low noise limit, and at the corrected logical levels, the second order terms are practically suppressed. In this limit, the PCa is on average more accurate than the CMC channels by a factor of 10^5.

TABLE VI. Thresholds for the Steane code under the ADC and its Pauli and expanded approximations. ADC/PCa uses ADC at the physical level and PCa at the logical level.

	Code capacity		Circuit-based	
Channel	$\langle\gamma_{th}\rangle$	RMS	$\langle\gamma_{th}\rangle \times 10^4$	RMS $\times 10^4$
ADC	0.18(17)	–	4.8(4.2)	–
PCa	0.132(38)	0.171	4.8(1.4)	3.91
PCw	0.061(43)	0.204	2.36(60)	4.69
CMCa	0.19(17)	0.0498	6.4(4.2)	1.67
CMCw	0.15(14)	0.0644	4.8(3.1)	1.12
DC	0.162(22)	0.165	7.2(1.4)	4.60
ADC/PCa	0.30(37)	0.255	4.9(4.2)	0.101

3. *High accuracy of the unconstrained PC*

For both the ADC and the $\mathrm{Pol}_{\pi/8}\mathrm{C}$, the unconstrained PC results in approximations that are honest (or almost honest) and extremely accurate at the logical corrected levels. In the limit of small error, this is very evident by comparing the quadratic coefficients of the PCa to the other approximations (See Tables III and V.). The high accuracy of the unconstrained PC in the context of EC has previously been observed. Geller and Zhou found very good agreement between the PCa or Pauli twirled approximation and two different realistic noise models when correcting a Bell state [22]. Likewise, Puzzuoli *et al.* observed great accuracy of the PCa when correcting a Choi state encoded in the [[5,1,3]] code [21]. As clearly explained in Ref. [21], after (perfect) EC, the process matrix elements corresponding to Pauli error strings that result in different syndromes become zero. Intuitively, we can say that the non-Pauli advantage of the expanded approximations at the physical level gets washed away after EC.

B. Level-one pseudothresholds

We perform the simulations of two different scenarios: (i) one with perfect EC, which results in a relatively high code-capacity pseudothreshold and (ii) one with faulty EC, which results in a more realistic circuit-based pseudothreshold. Apart from the average pseudothreshold, we also calculate the root mean square difference (RMS) between the pseudothresholds given by the target non-Clifford channel and the ones predicted by each approximate channel:

$$\mathrm{RMS} = \sqrt{\left\langle \left(\mathrm{p}_{th}^{\mathrm{channel}} - \mathrm{p}_{th}^{\mathrm{approx}}\right)^2 \right\rangle}. \tag{11}$$

The RMS quantifies the accuracy of each approximate channel to estimate the pseudothreshold of the target channel. We calculate the RMS because comparing only the average values does not account for any cancellation of errors. A certain approximate channel can do a very poor job at approximating the pseudothreshold for every initial state, but result in an average that is close to the target's average.

TABLE VII. Thresholds for the Steane code under the $\mathrm{Pol}_{\pi/8}\mathrm{C}$ and its Pauli and expanded approximations. $\mathrm{Pol}_{\pi/8}\mathrm{C/PCa}$ uses $\mathrm{Pol}_{\pi/8}\mathrm{C}$ at the physical level and PCa at the logical level.

	Code capacity		Circuit-based	
Channel	$\langle p_{th}\rangle$	RMS	$\langle p_{th}\rangle \times 10^4$	RMS $\times 10^4$
$\mathrm{Pol}_{\pi/8}\mathrm{C}$	0.14(24)	–	3.5(1.5)	–
PCa	0.086(74)	0.238	3.10(26)	1.53
PCw	0.078(16)	0.237	3.46(35)	1.48
CMCa	0.11(21)	0.112	3.09(85)	0.816
CMCw	0.09(14)	0.169	2.91(76)	0.991
DC	0.083(12)	0.244	3.92(64)	1.60
$\mathrm{Pol}_{\pi/8}\mathrm{C/PCa}$	0.14(25)	0.0255	3.5(1.5)	1.19×10^{-3}

The results for the ADC and the $\mathrm{Pol}_{\pi/8}\mathrm{C}$ are summarized in Tables VI and VII, respectively. For the ADC, the pseudothresholds are expressed in terms of the damping strength, γ, while for the $\mathrm{Pol}_{\pi/8}\mathrm{C}$, they are expressed in terms of the noise strength, p. In both cases, the standard deviation of the pseudothresholds is included inside parentheses. Notice that the code-capacity pseudothresholds are about 3 orders of magnitude higher than the circuit-based ones. The latter ones are on the range expected for the Steane code [30]. Although the code-capacity pseudothresholds are unrealistically high, they show similar trends with respect to their circuit-based counterparts.

As can be seen from Tables VI and VII, in general, the standard deviations of the pseudothresholds about its average values are high, especially for the target non-Clifford channels and its expanded approximations. Despite the fact that we consider relatively few initial states (80 and 20 for the code-capacity and circuit-based cases, respectively), the high variances are not a consequence of the small sample sizes. In fact, when reducing the sample size to only six initial points (the six Pauli states), the variances increase only slightly, and for some channels do not increase at all. Instead, the high variances are due to the extreme sensitivity of the pseudothreshold to the initial state. As an illustrative example, consider Fig. 5. The plot to the right shows how the circuit-based pseudothreshold of the ADC and its approximations varies as the initial state changes from $|0\rangle$ to $|1\rangle$ as a function of the angle θ. Notice, that the pseudothreshold for the ADC and its expanded approximations is particularly sensitive to the initial state, ranging from 0, when the initial state is the fixed point of the ADC, to $\sim 10^{-3}$.

It is interesting that the Pauli channels always result in pseudothresholds that are lower than the real ones. This trend has also been observed by Tomita and Svore on the surface code [6] and suggests that anisotropic Pauli channel approximations to realistic noise models are pessimistic. The CMCw approximations also result in lower pseudothresholds. This is in contrast to the isotropic Pauli channel approximation (DC) that yields optimistic pseudothresholds.

The CMCs give more accurate pseudothreshold estimates than the PCs, as can be seen by comparing their RMS values. Although we might expect the a channels to result in better approximations than the W channels, in general this is not the case. The most important variation is between the CMCs and the PCs. In general, however, the W channels result in lower pseudothresholds than the a channels, which implies that honest approximations at the physical level do a good job at giving conservative estimates of the threshold. Finally, we notice that the circuit-based pseudothresholds are quite comparable yielding pseudothresholds within a factor of two for all of the error models. The DC model representing isotropic depolarizing noise yields the worst results.

In the previous section, we noticed that the PCa, one of the simplest approximations at the physical level, and one that is not even honest, results in very accurate and practically

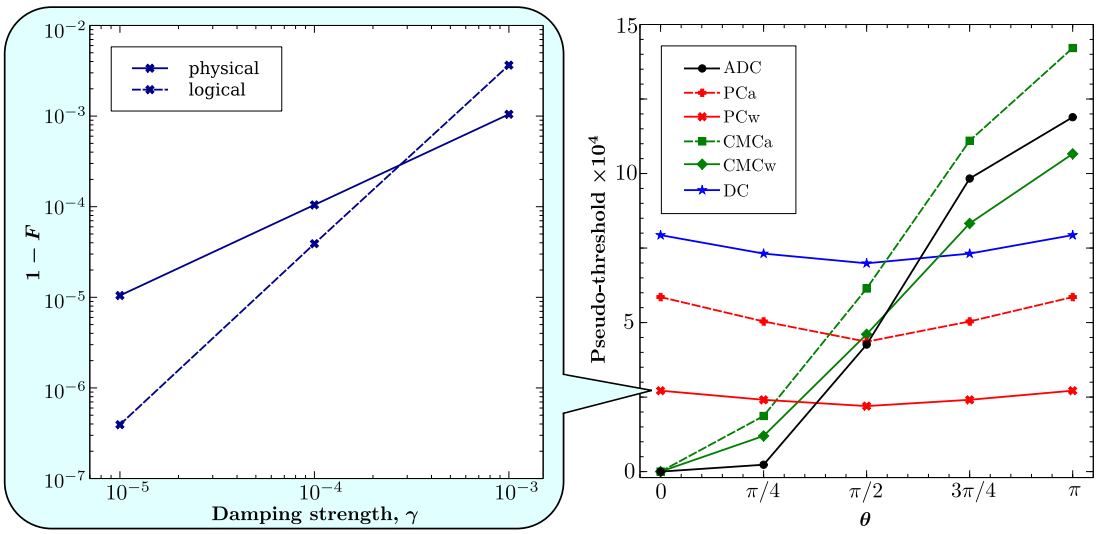

FIG. 5. (Color online) Variation of the circuit-based level-one pseudothreshold as a function of the angle θ for the ADC and its approximations. Each point corresponds to the pseudothreshold averaged over different values of the angle ϕ for the same angle θ. The initial state is given by $|\psi\rangle = \cos(\theta/2)|0\rangle + e^{i\phi}\sin(\theta/2)|1\rangle$. For the ADC and its expanded approximations, the pseudothreshold depends strongly on the initial state. The zoom-in figure on the left shows how the pseudothreshold is computed for a particular point on the Bloch sphere, namely by finding the first intersection between the physical and logical error $(1 - F)$.

honest approximations at the corrected logical levels. In the context of our level-one pseudothreshold estimation, this result suggests that we can take a different strategy. Instead of using the approximate channel at both the physical and logical level to calculate the pseudothreshold, we can use the target channel at the physical level and the PCa approximation at the logical level. More generally, we can simulate the realistic noise model in an exact way whenever it is feasible, and in the encoded cases just use the PCa. If we take this approach, we obtain more accurate state by state pseudothresholds for the circuit-based case as seen in Tables VI and VII.

VI. CONCLUSIONS

We have studied the feasibility of using approximate error channels at the physical level to simulate the performance of QEC protocols under the influence of nonstabilizer errors. We have selected the Steane [[7,1,3]] code as a model QEC protocol and have calculated the honesty and accuracy of the Pauli and expanded approximations to realistic nonstabilizer errors. We have also computed the code's pseudothreshold under the different error models.

Similar to results recently obtained for distance-3 surface codes [6], the PC approximations result in lower pseudothreshold values than the realistic error channels. In contrast, the isotropic DC approximation yields higher pseudothresholds than the target channels in the circuit-based model. Since most thresholds in the literature use two-qubit and one-qubit depolarizing channels, we expect that realistic error models with equivalent fidelity will have slightly lower pseudothresholds in practice. However, for more realistic models including correlated errors across qubits [4,31], it is unclear whether the observed trends in honesty and accuracy will be maintained.

We have also found that physically honest approximations compose well: they result in honest approximations at the logical level. Perhaps more interestingly, for both realistic noise models analyzed, the dishonesty of the PCa gets greatly reduced at the corrected logical levels and its accuracy becomes extremely high. This suggests that the best protocol is to model the error as realistically as possible at the physical level and use the PCa at the logical level. Although we have focused on the Steane code with Shor EC, the high accuracy of the PCa at the logical level will most likely hold for any QECC that discretizes errors to Pauli operators. This includes all stabilizer codes. It should also hold for other EC protocols that rely on ancillary stabilizer states to detect Pauli errors, including Steane and Knill EC [13,32].

As explained by Puzzuoli *et al.* [21], single-qubit errors can be separated into errors that deform the Bloch sphere (nonunitary) and errors that preserve it (unitary). Both target error models analyzed in our work belong to the deforming regime, where the PCa yields effectively honest approximations at the logical level for small errors. Puzzuoli *et al.* found that when the errors are unitary, the PCa generally results in very dishonest approximations. In future work, we will compute the level-one pseudothreshold for the Steane and other codes under unitary errors, to determine if our Pauli and expanded approximations still result in pessimistic pseudothreshold estimates.

ACKNOWLEDGMENTS

We thank Colin Trout and Chingiz Kabytayev for helpful comments and CT for helping to prepare Fig. 5. This research was funded by the Office of the Director of National Intelligence (ODNI), Intelligence Advanced Research Projects Activity (IARPA), through the Army Research Office grant W911NF-10-1-0231. All statements of fact, opinion or conclusions contained herein are those of the authors and should not be construed as representing the official views or policies of IARPA, the ODNI, or the U.S. Government.

[1] D. Poulin, Phys. Rev. A **74**, 052333 (2006).
[2] H. Goto and H. Uchikawa, Sci. Rep. **3**, 2044 (2013).
[3] M. Suchara, A. W. Cross, and J. M. Gambetta, arXiv:1410.8562 [quant-ph].
[4] E. Novais and E. R. Mucciolo, Phys. Rev. Lett. **110**, 010502 (2013).
[5] A. G. Fowler, Phys. Rev. A **88**, 042308 (2013).
[6] Y. Tomita and K. M. Svore, Phys. Rev. A **90**, 062320 (2014).
[7] P. Jouzdani, E. Novais, I. S. Tupitsyn, and E. R. Mucciolo, Phys. Rev. A **90**, 042315 (2014).
[8] D. Gottesman, Ph.D. thesis, California Institute of Technology, 1997, http://resolver.caltech.edu/CaltechETD:etd-07162004-113028.
[9] S. Aaronson and D. Gottesman, Phys. Rev. A **70**, 052328 (2004).
[10] E. Magesan, D. Puzzuoli, C. E. Granade, and D. G. Cory, Phys. Rev. A **87**, 012324 (2013).
[11] M. Gutiérrez, L. Svec, A. Vargo, and K. R. Brown, Phys. Rev. A **87**, 030302 (2013).
[12] A. M. Steane, Phys. Rev. Lett. **77**, 793 (1996).
[13] A. M. Steane, Phys. Rev. A **68**, 042322 (2003).
[14] K. M. Svore, D. P. DiVincenzo, and B. M. Terhal, Quantum Inf. Comput. **7**, 297 (2007).
[15] T. S. Metodi, D. D. Thaker, A. W. Cross, F. T. Chong, and I. L. Chuang, in *Proceedings of the 38th Annual IEEE/ACM International Symposium on Microarchitecture 12–16 November 2005, MICRO-38* (IEEE Computer Society, Washington, DC, USA, 2005), pp. 305–316.
[16] Y. Tomita, M. Gutiérrez, C. Kabytayev, K. R. Brown, M. R. Hutsel, A. P. Morris, K. E. Stevens, and G. Mohler, Phys. Rev. A **88**, 042336 (2013).
[17] Y. S. Weinstein, Phys. Rev. A **89**, 020301 (2014).
[18] A. Abu-Nada, B. Fortescue, and M. Byrd, Phys. Rev. A **89**, 062304 (2014).
[19] J. T. Anderson, G. Duclos-Cianci, and D. Poulin, Phys. Rev. Lett. **113**, 080501 (2014).
[20] D. Nigg, M. Müller, E. A. Martinez, P. Schindler, M. Hennrich, T. Monz, M. A. Martin-Delgado, and R. Blatt, Science **345**, 302 (2014).

[21] D. Puzzuoli, C. E. Granade, H. Haas, B. Criger, E. Magesan, and D. G. Cory, Phys. Rev. A **89**, 022306 (2014).
[22] M. R. Geller and Z. Zhou, Phys. Rev. A **88**, 012314 (2013).
[23] W. van Dam and M. Howard, Phys. Rev. Lett. **103**, 170504 (2009).
[24] M. D. Grace, J. Dominy, R. L. Kosut, C. Brif, and H. Rabitz, New J. Phys. **12**, 015001 (2010).
[25] A. Gilchrist, N. K. Langford, and M. A. Nielsen, Phys. Rev. A **71**, 062310 (2005).
[26] I. L. Chuang and M. A. Nielsen, J. Mod. Opt. **44**, 2455 (1997).
[27] P. Aliferis, D. Gottesman, and J. Preskill, Quantum Inf. Comput. **6**, 97 (2006).
[28] A. W. Cross, D. P. DiVincenzo, and B. M. Terhal, Quantum Inf. Comput. **9**, 541 (2009).
[29] D. P. DiVincenzo and P. W. Shor, Phys. Rev. Lett. **77**, 3260 (1996).
[30] A. M. Steane, Fortsch. Phys. **46**, 443 (1998).
[31] A. G. Fowler and J. M. Martinis, Phys. Rev. A **89**, 032316 (2014).
[32] E. Knill, Nature **434**, 39 (2005).